Sensors and Actuators 73 (1999) 45–51

A new silicon rate gyroscope

W. Geiger *, B. Folkmer, J. Merz, H. Sandmaier, W. Lang

Hahn-Schickard-Gesellschaft, Institute of Micromachining and Information Technology, HSG-IMIT, Wilhelm-Schickard-Str. 10, D-78052 Villingen-Schwenningen, Germany

Received 13 April 1998; accepted 7 October 1998

Abstract

A new silicon rate gyroscope of small size, low cost, and high performance is described. The device is called MARS-RR, which means *M*icromachined *A*ngular *R*ate *S*ensor with *two R*otary oscillation modes. First prototypes, MARS-RR1 yielded random walk and bias stability as low as 0.14 deg/h and 65 deg/h, respectively. The rate equivalent rms noise corresponds to a resolution of 0.05 deg/s in a 50 Hz bandwidth. This performance is achieved by a new sensor design featuring decoupling of the actuation and the detection oscillation modes. Because of decoupling, the modes mechanical and electromechanical crosstalk, one main error source of micromachined gyros, can be reduced and therefore the zero rate output (ZRO) almost disappears. Despite the small sensor area of 6 mm^2, the detection capacitance amounts to approximately 3 pF. Thus, subatomic deflections are detectable and a high sensitivity is achieved. MARS-RR1 was manufactured within the Bosch Foundry process [M. Illing, Micromachining Foundry Designrules, Version 1.0, Bosch Mikroelektronik; M. Offenberg, H. Münzel, D. Schubert, B. Maihöfer, F. Lärmer, E. Müller, O. Schatz, J. Marek, SAE Technical Paper Series, 960758, SAE 96, The Engineering Society for Advancing Mobility Land Sea Air and Space, 1996, reprinted from Sensors and Actuators, 1996 (SP-1133), p. 35; M. Offenberg, F. Lärmer, B. Elsner, H. Münzel, W. Riethmüller, Novel Process for a Monolithical Integrated Accelerometer, Transducer '95, Eurosensor IX, 148-C4, pp. 589–592] and therefore it was possible for us to reduce the development time considerably.

Keywords: Gyroscope; Angular rate sensor; Angular velocity

1. Introduction

During the last couple of years, great interest has turned up in the production of a low-cost rate gyroscope and, in order to put this idea into practice, the micromachining technologies are being investigated [4–7]. The development of vibratory gyroscopes fabricated by silicon technologies now has a tendency to use 'surface micromachining like processes' with increasing film thickness of the layer containing the mechanical structure to achieve higher inertial mass and capacitance.

Within these technologies, comb-drives are usually used to force an oscillation of the mechanical structure [8–10]. By turning the device Coriolis forces generate a second oscillation perpendicular to the first one with an amplitude proportional to the angular rate. Respectively, these oscillations or modes are referred to as the primary and the secondary motion.

The main sources of errors of comb driven gyroscopes are mechanical and electromechanical coupling effects and the small deflections which are to be measured. The last mentioned problem has to be solved by using a detection capacitance as large as possible. The coupling effects include purely mechanical crosstalk and at least two electromechanical effects.

First of all, due to the substrate supporting the comb-drives, the electric field is unsymmetric and electrostatic forces arise, which pull the mechanical structure upwards. This electromechanical coupling effect is called levitation [11].

Secondly, if the comb drives are not decoupled from the secondary oscillation, the overlap of a pair of combs changes in dependence of the input rate. Thus, the driving forces change and a nonlinear behaviour results.

MARS-RR was designed in a way that a large detection capacitance allows very sensitive measurement and that the mentioned coupling effects are reduced to a great extent.

* Corresponding author. Tel.: +49-7721-943-226; Fax: +49-7721-943-210; E-mail: wolfram.geiger@imit.uni-stuttgart.de

0924-4247/99/$ - see front matter
PII: S0924-4247(98)00253-2

2. Theory of operation

Fig. 1 shows a schematic drawing of MARS-RR. The mechanical sensor element consists of comb drives, which build the spokes of the inner wheel, and an outer rectangular structure, which is called secondary oscillator. The entire movable structure is electrostatically driven to a rotary oscillation around the z-axis by four comb drives (primary mode). The remaining four comb capacitors are used to detect the primary oscillation. When the device is turned around its sensitive axis, the x-axis, Coriolis forces arise, which cause a rotary oscillation around the y-axis (secondary mode). In this direction, the high stiffness of the beam suspension suppresses an oscillation of the inner wheel. Only the rectangular structure can follow the Coriolis forces, because it is decoupled from the inner wheel by torsional springs. The oscillation of the secondary oscillator around the y-axis is capacitively detected by substrate electrodes.

The suppression of an out of plane motion of the inner wheel prevents any changes of the overlap of the combs in z-direction. Thus, undesired changes of the driving force are suppressed, which would yield a nonlinear output characteristics.

As pointed out in Ref. [12], the use of eight pairs of combs and their proper, highly symmetrical arrangement compensates the levitation forces up to second order. Terms of higher order are effectively suppressed by the decoupling and the high stiffness of the suspension beams in z-direction.

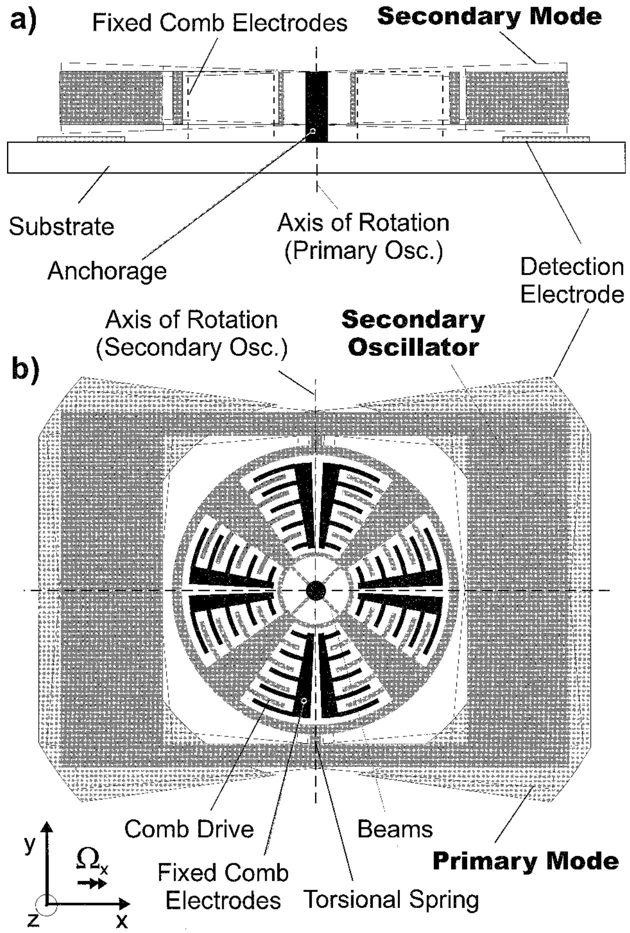

Fig. 1. (a) Cross-section and (b) top view of the angular rate sensor MARS-RR. A ZRO is prevented by the circular detection electrodes as long as the misalignment of the movable structure and the detection electrodes is zero.

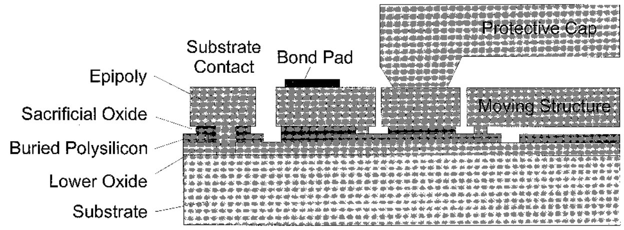

Fig. 2. Layer structure of the Bosch Foundry Process [1].

3. Fabrication

MARS-RR1 was produced within the Bosch Foundry process [1–3], which is a process similar to conventional surface micromachining with an additional protective silicon cap (Fig. 2). ''This process features a polycrystalline silicon layer with a thickness of 10.3 μm for the freestanding structure. The large thickness is achieved by using an epitaxial deposition of polysilicon ('epipoly'). A special trench technique allows the formation of vertical sidewalls with high aspect ratio. In addition to the functional polysilicon layer a second thin poly-Si-layer ('buried poly') is provided underneath, which serves as interconnect, shield or counter-electrode. The buried poly layer is isolated from the epipoly by the sacrificial oxide and from the substrate by a lower oxide'' [1].

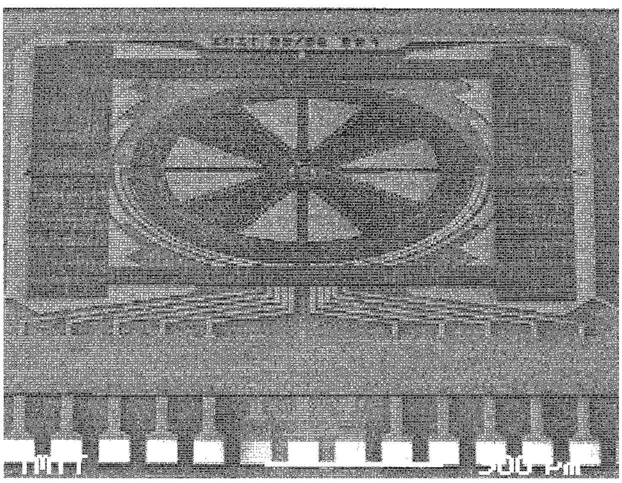

Fig. 3. SEM of the angular rate sensor MARS-RR1.

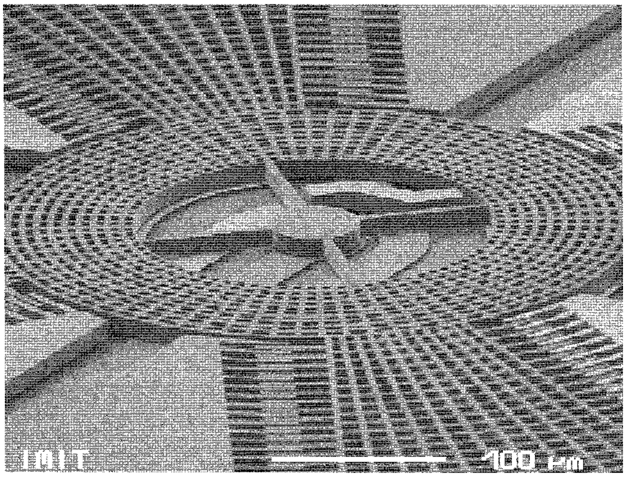

Fig. 4. SEM of the angular rate sensor MARS-RR1 showing the anchorage and a crossing of interconnections.

Micrographs of the realized sensor are shown in Figs. 3 and 4.

4. Readout technique

The readout of the secondary oscillation is accomplished by exciting the substrate electrodes with 1 MHz ($=\omega_{CS}$), 4 V_{pp} carrier signals. By a flip-flop circuitry, the complementary carrier signals are generated. When the secondary oscillator is not oscillating around the *y*-axis, the secondary capacitors are balanced and there is no net signal at the input node of the operational amplifier (node 1 in Fig. 5). When the secondary oscillator is driven by Coriolis forces, its capacitors become unbalanced and the carrier signal with an amplitude modulated by the mechanical oscillator's motion appears at node 1. After a first demodulation with the carrier frequency, a low frequency signal corresponding to the mechanical motion of the secondary oscillator appears at node 2. The second demodulation with the drive frequency yields a DC voltage proportional to the input rate.

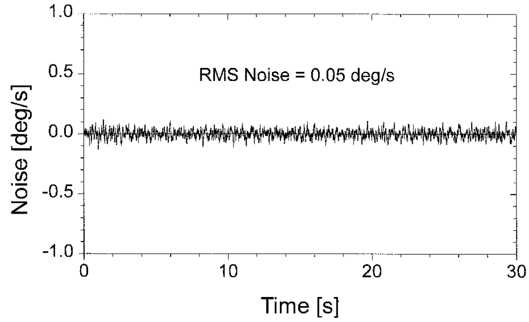

Fig. 6. Short term noise of MARS-RR1 at zero rate input in a bandwidth from 0 Hz to 50 Hz.

The readout of the primary oscillation is realized by the same technique but with 1.2 MHZ ($=\omega_{CP}$), 1 V_{pp} carrier signals to separate the signals corresponding to the two oscillation. The carrier signals are applied to the two diagonally placed pairs of comb capacitors.

For driving the primary oscillation complementary 3 V_{pp} signals with an offset of 1.5 V are applied to the two pairs of comb drives. A high pass filter (HPF) reduces electrical crosstalk of the driving voltage to the output signals.

The measurements are made without any frequency matching.

5. Test results

Tests were carried through with the sensor placed in a vacuum chamber at a pressure of 10^{-2} mbar. The turn table inside the chamber is connected to the outside motor by a ferrofluidics feedthrough. The electrical signals are transmitted by slip rings.

Fig. 6 shows the sensor noise at zero rate input measured using a low pass filter first order with a corner

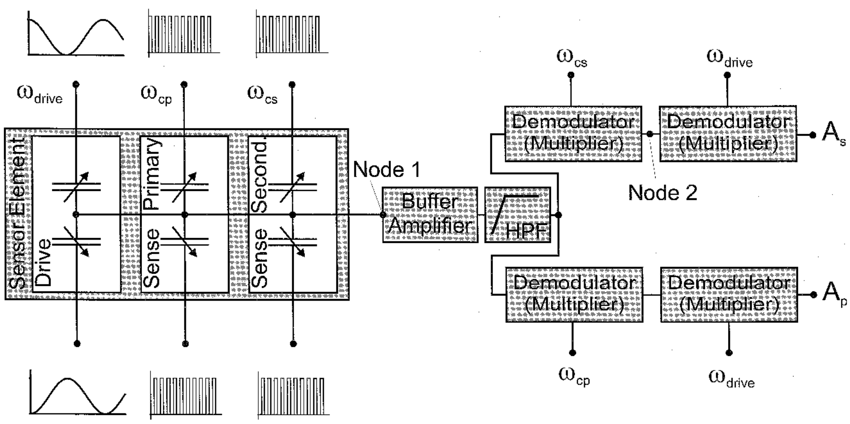

Fig. 5. Schematics of the electronics used with the angular rate sensor MARS-RR.

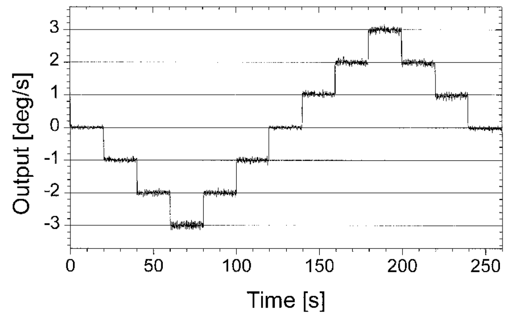

Fig. 7. Response to ±1 deg/s steps of the input rate. The noise is mainly due to crosstalk of the motor electronic signals.

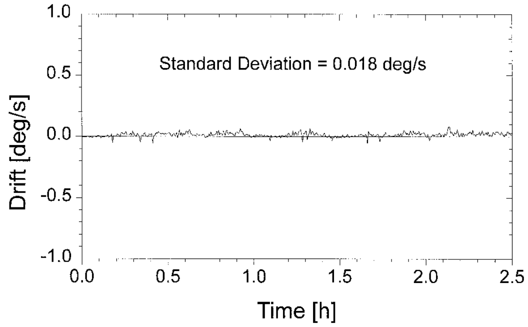

Fig. 8. Offset drift of MARS-RR1 at zero input rate measured over a period of 2.5 h.

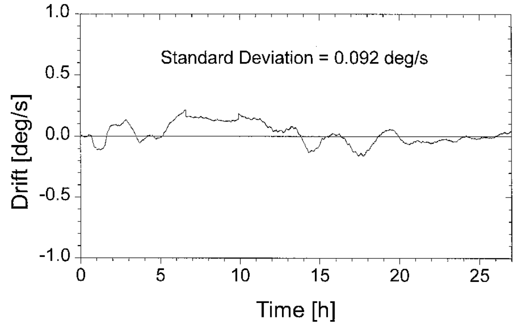

Fig. 9. Offset drift of MARS-RR1 at zero input rate measured over a period of 27 h.

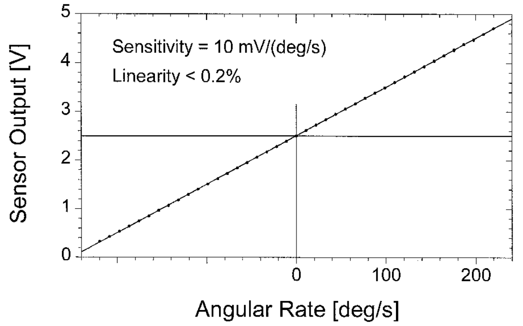

Fig. 10. Sensor output vs. rate input. The integration time is 1 s for each measured point. The linearity is calculated with the end point straight line method.

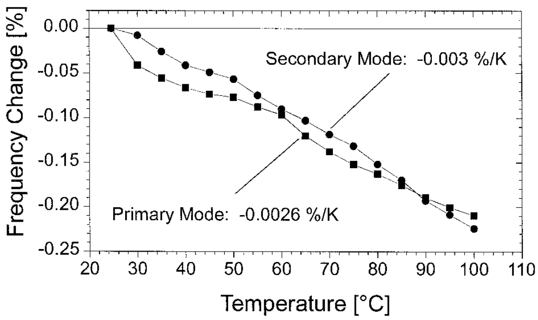

Fig. 11. Resonance frequency change of the primary and the secondary mode with temperature.

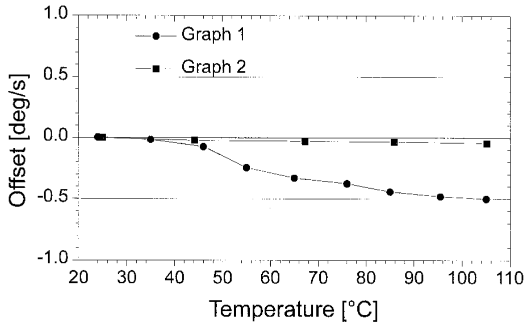

Fig. 12. Temperature dependence of the offset at zero input rate; graph 2 with compensation.

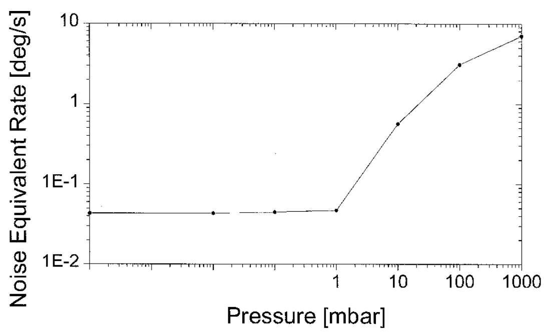

Fig. 13. Pressure dependence of the noise equivalent rate in a 50-Hz bandwidth. The driving voltage is 10 V_{pp}.

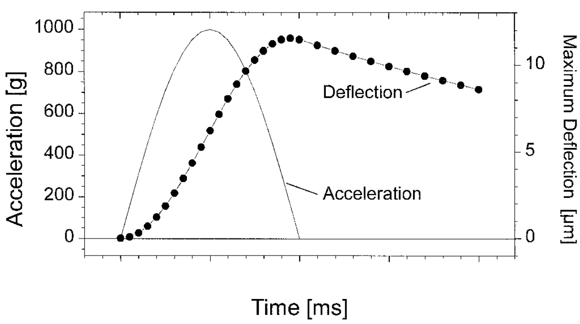

Fig. 14. FEM analysis of the maximum deflection at a 1000 g's shock perpendicular to the substrate.

frequency of 50 Hz. The rms noise corresponds to a resolution of 0.05 deg/s. The measurement corresponding to Fig. 6 was made with the motor of the turn table switched off, because the electric motor signals are disturbing the sensor signals severely.

Fig. 7 shows the sensor output for steps of ±1 deg/s. With the motor switched on the rms sensor noise amounts to approximately 0.15–0.20 deg/s.

The sensor drift is shown in Fig. 8. For the displayed time of 2.5 h the standard deviation of the drift amounts to 0.018 deg/s or 65 deg/h. Fig. 9 shows the long term drift of 27 h. The standard deviation as well as the peak values are larger as in Fig. 8 but still show a very good center line.

Measurements of the sensor output vs. the rate input are shown in Fig. 10. The sensitivity is adjusted to 8 mV/(deg/s) with a sensor output of 2.5 V at zero rate input. Calculating the linearity based on the end point straight line method measured at the midrange input rate yields a linearity smaller than 0.3% full scale span.

Measurements of the temperature dependence of the natural mechanical resonance frequencies show a very small temperature coefficient (Fig. 11). Therefore, it is expected that the small temperature dependence of the offset (0.5 deg/s for 25–105°C, see Fig. 12, graph 1) is mainly due to the readout electronics. Experiments with a very simple compensation (Fig. 12, graph 2) indicate that an offset change much smaller than 0.1 deg/s is possible.

As already mentioned, the measurements above were performed at a pressure of 10^{-2} mbar. Further reducing the pressure results in a higher quality factor and smaller Brownian noise. On principle, this enables better sensor performance or allows for the same performance with smaller sensor dimensions. The primary amplitude of MARS-RR is restricted to 1 deg by stoppers, which are used as overload protection and for controlling the vibration amplitude without an electrical control circuit. With a driving voltage of 10 V_{pp} this maximum deflection is achieved for pressures up to approximately 1 mbar. Since the Brownian noise is not the dominant noise source the sensor performance stays constant (Fig. 13). At higher pressures, the vibration amplitude, and with it the sensitivity, decrease resulting in worse resolution. In the range from 1 mbar to 10 mbar the noise equivalent rate increases form 0.05 to 0.5 deg/s. At 1 bar, it amounts to approximately 7 deg/s. The pressure dependence shows that even at moderate vacuum, a high resolution is obtained, which may be important with respect to reliable vacuum packaging of the sensor. In comparison with other micromachined gyros, the high pressures are possible because of the comparably high mass and moment of inertia, which keep the Brownian noise small.

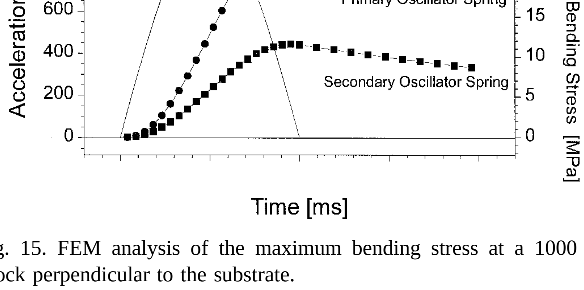

Fig. 15. FEM analysis of the maximum bending stress at a 1000 g's shock perpendicular to the substrate.

Table 1
Technical data of MARS-RR1

Technical data	MARS-RR
Performance	
Bias stability (1 σ)	0.018 deg/s = 65 deg/h
Noise (1 σ)	0.0024 deg/s/$\sqrt{Hz}$ = 0.14 deg/$\sqrt{h}$
Noise equivalent rate in 50-Hz bandwidth (rms)	0.05 deg/s
Dynamic range	±300 deg/s
Sensitivity	8 mV/(deg/s)
Linearity (end point straight line)	< 0.3%
Power supply (temporary)	
Supply voltage	15 V
Current (discrete electronics)	20 mA
Environment	
Bias stability (25–105)°C	< 0.5 deg/s
Shock survival (1 ms, 1/2 sine)	1000 g (FEM-Model)
Acceleration error	
x-axis	< 2E-4 (deg/s)/g (FEM-Model)
y-axis	< 1E-5 (deg/s)/g (FEM-Model)
z-axis	< 1 s_m (deg/s)/g (FEM-Model)

Finite element modelling of a 1000 g's shock (1 ms, 1/2 sine) yield a maximum deflection of 11.54 μm (Fig. 14) and a maximum stress of 25.4 MPa (Fig. 15) which is clearly below the fracture stress of silicon (approximately 100–700 MPa [13,14]). First drop tests have confirmed the simulations.

The first, the second, and the third sensor modes are rotary oscillation modes around the *y*-, the *z*- and the *x*-axis, respectively. Linear accelerations are therefore effectively compensated. The fourth mode is a linear one in *z*-direction ('flying mode'). The measured resonance frequencies of 975 Hz, 1420 Hz, 1970 Hz and 2390 Hz correspond to the FEM-simulated frequencies of 990 Hz, 1428 Hz, 2065 Hz and 2166 Hz within approximately 10%. Simulations of applied *x*- and *y*- accelerations yield deflections in the order of 4E-5 μm/g at 1420 Hz. This corresponds to an *x*-acceleration error of 2E-4 (deg/s)/g and a *y*-acceleration error smaller than 1E-5 (deg/s)/g. These values can be reduced by changing the design of the detection electrodes. With the present design, the most severe problem regarding the z-acceleration is a misalignment s_m of the buried polysilicon layer and the epipoly layer. This misalignment disturbs the symmetry of the detection electrodes and can lead to an acceleration error, provided that the frequency of the acceleration is equivalent to the frequency of the primary mode (1420 Hz). At this frequency, FEM simulations yield a deflection in z-direction of approximately 0.1 μm/g which results in a worst case z-acceleration error of approximately 1 s_m (deg/s)/g, with the misalignment s_m given in microns. For applications in which vibrations with amplitudes of 1 g occur in the range of 1400 Hz, this acceleration error has to be reduced by a more tolerant design of the detection electrodes. This way, it will be possible to obtain an z-acceleration error smaller than 0.01 s_m (deg/s)/g. With $s_m = 1$ μm, the acceleration error then will be below the resolution even for accelerations with amplitudes of 5 g at 1420 Hz.

The measured and simulated parameters are summarized in Table 1.

6. Conclusion

MARS-RR1 was designed to overcome the main drawbacks of micromachined comb driven rate gyroscopes. The outstanding performance of the device proves the conceptual approach. Our further work on MARS-RR1 will concentrate on packaging and the readout electronics to develop a sensor ready for production. The applications are, among others, advanced airbag systems, active suspension, and navigation.

Acknowledgements

We sincerely appreciate that the device is manufactured by Robert Bosch within the Bosch Foundry process and we wish to express our special thanks to M. Illing for his permanent assistance. The finite element modelling done by N. Hey and S. Messner has contributed a great deal to the success of the project. Furthermore, we would like to thank M. Kieninger and M. Pascal for making the measurements.

References

[1] M. Illing, Micromachining Foundry Designrules, Version 1.0, Bosch Mikroelektronik.

[2] M. Offenberg, H. Münzel, D. Schubert, B. Maihöfer, F. Lärmer, E. Müller, O. Schatz, J. Marek, SAE Technical Paper Series, 960758, SAE 96, The Engineering Society for Advancing Mobility Land Sea Air and Space, 1996, reprinted from Sensors and Actuators 1996 (SP-1133), p. 35.

[3] M. Offenberg, F. Lärmer, B. Elsner, H. Münzel, W. Riethmüller, Novel Process for a Monolithical Integrated Accelerometer, Transducer '95, Eurosensor IX, 148-C4, pp. 589–592.

[4] I.D. Hopkin, Vibrating Gyroscopes, Symposium Gyro Technology 1997, Stuttgart, Germany, September 1997, pp. 1.0–1.10.

[5] F. Paoletti, M.-A. Grétillat, N.F. de Rooij, A Silicon Micromachined Vibrating Gyroscope with Piezoresistive Detection and Electromagnetic Excitation, Proc. IEEE Micro Electromechanical Systems Conference, San Diego, CA, USA, February 1996, pp. 162–167.

[6] R. Voss, K. Bauer, W. Ficker, T. Gleissner, W. Kupke, M. Rose, S. Sassen, J. Schalk, H. Seidel, E. Stenzel, Silicon Angular Rate Sensor for Automotive Applications with Piezoelectric Drive and Piezoresistive Read-Out, Tech. Digest, 9th Int. Conf. Solid-State Sensors and Actuators (Transducers '97), Chicago, IL, USA, June 1997, pp. 879–882.

[7] M. Lutz, W. Golderer, J. Gerstenmeier, J. Marek, B. Maihöfer, S. Mahler, H. Münzel, U. Bischof, A Precision Yaw Rate Sensor in Silicon Micromachining, Tech. Digest, 9th Int. Conf. Solid-State Sensors and Actuators (Transducers '97), Chicago, IL, USA, June 1997, pp. 847–850.

[8] J. Bernstein, S. Cho, A.T. King, A. Kourepins, P. Maciel, M. Weinberg, A Micromachined Comb-Drive Tuning Fork Rate Gyroscope, Proc. IEEE Micro Electromechanical Systems Conference, FL, USA, February 1993, pp. 143–148.

[9] K. Funk, A. Schilp, M. Offenberg, B. Elsner, F. Lärmer, Surface-micromachining of Resonant Silicon Structures, 8th International Conference on Solid-State Sensors and Actuators (Transducers '95/Eurosensors IX), Stockholm, Sweden, 25–29 June, 1995, Late News, pp. 50–52.

[10] K. Tanaka, Y. Mochida, M. Sugimoto, K. Moriya, T. Hasegawa, K. Atsuchi, K. Ohwada, A micromachined vibrating gyroscope, Sensors and Actuators A 50 (1995) 111–115.

[11] W.C. Tang, M.G. Lim, R.T. Howe, Electrostatic comb drive levitation and control method, Journal of Microelectromechanical Systems 1 (4) (1992) .

[12] W. Geiger, B. Folkmer, U. Sobe, H. Sandmaier, W. Lang, New designs of micromachined vibrating rate gyroscopes with decoupled oscillation modes, Sensors and Actuators A 66 (1–3) (1998) 118–124.

[13] R. Kassing, I. Rangelow, Silizium f.d. Mikromechanik, Fachbeilage Mikroperipherik, VDI/VDE, Berlin, Okt. 1988.

[14] M. Paulsen, Wacker-Silizium Wafer Produktinformation, Wacker-Chemitronic, D-82633 Burghausen, April 1992.

Wolfram Geiger studied Physics at the University of Tübingen, Germany, and the University of Arizona, Tucson, USA. He received his Diploma on an electrostatically driven micropump from the University of Tübingen in 1994. From 1994 to 1996 he was working at the Fraunhofer-Institute of Microelectronic Circuits and Systems (IMS) in Dresden, where he was engaged in research on SIMOX based accelerometers. Since joining HSG-IMIT in 1996, he works on high resolution micromachined rate gyroscopes. The main topics of his work are design, process development, electronics and measuring methods.

Bernd Folkmer received his Diploma degree in Mechanical Engineering from the Technical University of Munich in 1990. He joined the Fraunhofer Institute for Solid State Technology, where he worked on various areas of MEMS simulation and development. Since 1995 he has been employed at the Hahn-Schickard Institute of Micromachining and Information Technology HSG-IMIT. His present interest is mechanical microsensor development in cooperation with SMEs.

Jürgen Merz joins since 1990 the HSG-IMIT. He develops electronic signal processing devices for micromechanical sensors and actuators. In an engineering study at the Feintechnikschule-Schwenningen from 1988 to 1990, he graduated as Technical Engineer of Electronics. His first job was as a dealer of consumer electronics from 1984 to 1988. He repaired electronic equipments. He joined the College of Further Education from 1981 to 1984 and graduated with communication electronics.

Hermann Sandmaier was born in Ruhstorf, Germany, in 1955. He received his MS and PhD degrees in Electrical Engineering from Munich Technical University in 1982 and 1988, respectively. He was working with the Fraunhofer Institute in Munich from 1982 to 1995, developing microsensors for physical and chemical quantities as well as microfluidic devices. He is currently the head of the Institute of Micromachining and Information Technology, a research center of German ‘Hahn-Schickard’ Society, and a professor at Stuttgart University. His research interest focuses on microsensors, microfluidics, microoptics, and microelectromechanical systems besides topics in technology, fabrication, and modelling. He received the Schlumberger Award in 1989. He is an Editorial Board Member of the Journal of Micromechanics and Microengineering as well as Sensors and Materials and Program Committee Member of MEMS-Workshop and Eurosensors.

Walter Lang studied Physics at Munich University and received his Diploma in 1982 on Raman spectroscopy of crystals with low symmetry. His PhD in Engineering at Munich Technical University was on flame-induced vibrations. In 1987, he joined the Fraunhofer Institute for Solid State Technology in Munich. In 1995, he became the head of the sensors department at the Institute of Micromachining and Information Technology HSG-IMIT in Villingen-Schwenningen, Germany. His areas of work are research and development in the field of sensors and measurement systems for angular rate, flow, pressure, and microswitches.